Surface structure of lithium-doped potassium tantalate using helium atom scattering

Rifat Fatema,* David H. Van Winkle,† and J. G. Skofronick
Department of Physics, Florida State University, Tallahassee, Florida 32306-4350, USA

Sanford A. Safron
Department of Chemistry and Biochemistry, Florida State University, Tallahassee, Florida 32306-4390, USA

F. A. Flaherty
Department of Physics, Valdosta State University, Valdosta, Georgia 31698-0055, USA

L. A. Boatner
Oak Ridge National Laboratory, Oak Ridge, Tennessee 37831, USA
(Received 2 October 2012; published 13 February 2013)

The structures of the (001) surface of potassium tantalate doped with nominally 2%, 4%, and 7% lithium have been investigated using high-resolution helium atom scattering. The surfaces were prepared by cleaving single-crystal samples *in situ* under UHV conditions. Diffraction measurements in the region around the He specular reflection angle soon after cleaving yielded specular peaks initially with broad shoulders. However, over a period of about an hour, the shoulders diminished into the background. Drift spectra measurements of the stabilized surfaces revealed that the step heights separating surface terraces were predominantly multiples of the approximately 4-Å unit-cell dimension rather than multiples of the approximately 2-Å half-unit-cell dimension expected from the cleaving of these crystals. Together, these results suggest that these surfaces are rapidly modified after cleaving by migration of ions to the surface from the near surface. Further, half-order diffraction peaks were observed in the ⟨100⟩ azimuth a short time after cleaving samples at room temperature, indicating that domains with (2×1) structure had formed.

DOI: 10.1103/PhysRevB.87.085419 PACS number(s): 68.49.Bc, 68.35.B−, 68.47.Gh

I. INTRODUCTION

Complex oxides, particularly at interfaces and in thin films, exhibit a variety of interesting and potentially useful phenomena which can be induced by temperature, film thickness, and compositional variation.[1,2] A short list of these includes magnetic and ferroelectric properties, electrical conductivity, and superconductivity.[1–3] Understanding their surface behavior is key to exploiting the properties of these materials. The bulk structures of several oxide perovskites relevant to this work have been investigated extensively.[4–21] Helium atom scattering (HAS) experiments have been reported from this laboratory on the surface structure and dynamics of the perovskites potassium tantalate (KT)[22,23] and potassium tantalate doped with niobium (KTN) over a range of concentrations.[24–26] A theoretical study of the surface of KT has also been reported.[27] Finally, a HAS investigation of the fluoride perovskite $KMnF_3$ allows for a comparison between the fluoride and oxide results.[28]

In this paper, we present the results of HAS experiments on potassium tantalate doped with lithium (KLT). The principal difference between the niobium and lithium dopants is that in the bulk, the Nb^{5+} ion replaces the Ta^{5+} ion which is surrounded by an octahedron defined by the six O^{2-} ions, whereas the Li^+ ions replace K^+ ions at a corner of some unit cells.[5,16,19] Other laboratories have shown that in the bulk, the small Li^+ ion is able to "hop" among six equivalent sites displaced in the ⟨100⟩ directions by about 1.2 Å from the K^+ corner position.[5,19] In the temperature range of our studies, bulk KLT is suggested to form nearly correlated polar clusters that are needlelike in shape and fluctuate around the ⟨100⟩ azimuth.[12] Because the Li^+ ions are off center in KLT, they form dipole moments and the materials are called random dipole ferroelectrics; they exhibit slow relaxation and are identified as relaxors.[13,14] At the surface, these displacements are probably somewhat modified and create localized dipole and quadrupole electric moments.

In HAS studies, domains with (2×1) structure have been observed to form on the (001) surfaces of KT and KTN after thermal cycling to low temperatures.[23–26] These may be related to the polar nanoregions (PNRs) observed in the bulk materials, which are thought to arise from electric moments associated with defects.[6,7,10,12,13,16–21] In these KLT studies, (2×1) domains form soon after cleaving even at room temperature, likely because of electric moments arising from the Li^+ displacements.

In the HAS experiments with KT and KTNs, the growth of the specular peak and decrease of the shoulders soon after cleaving and the observation of terrace step heights in multiples of the unit-cell dimension were ascribed to migration of potassium and oxygen ions to the surface from the near-surface bulk.[29,30] For the 30% Nb-doped KTN, the shoulders on the specular peak were too small to quantify in this way. Such migration from the bulk to the surface of the A and O ions in ABO_3 perovskites has been reported at high temperatures.[30] The similar observations reported in this work for KLT were consistent with the previous results.

The He diffraction characterizing the metastable behavior of KLT is well described by a treatment based on the work of Croset and de Beauvais,[31] as in the case reported previously for KT.[29] For KLT, the time dependence of the coverage of

 ©2013 American Physical Society

the surface by the migrating ions, as monitored by the He diffraction, is consistent with a simple kinetic model. The earlier results for KT are also accurately fit by this model.

A brief description of the apparatus and experiments carried out is given in the next section, followed by the results of the experiments. The results are then discussed and the conclusions highlighted.

II. HAS INSTRUMENT AND EXPERIMENTS

The FSU HAS instrument has been described in considerable detail in previous publications from this laboratory.[22,23,25,32] Briefly, the instrument consists of three main sections: (i) the beam source chamber, (ii) the scattering chamber, and (iii) the time-of-flight (TOF) and detector chambers. A nearly monoenergetic ($\Delta E/E \approx 2\%$ or $\Delta v/v \approx 1\%$) helium atom beam is produced by expanding helium gas at 25–30 bar pressure through a nominal 30-μm nozzle, and then passing it through a 1-mm-diameter skimmer. The temperature of the nozzle can be varied from about 80 to 325 K, resulting in He atom energies ranging from approximately 20 to 70 meV. The beam passes through a differentially pumped region before entering the scattering chamber and striking the sample at an incident angle θ_i measured with respect to the surface normal of the sample.

The He atoms scatter from the sample in all directions. Those reflected in the plane defined by the nozzle-to-sample and sample-to-detector axes are able to travel through the TOF section to the detector. The geometry of the instrument fixes the intersection of these axes to be at 90° so that, measured with respect to the surface normal, the incident and scattering angles of the detected atoms satisfy $\theta_f = 90°\text{-}\theta_i$. The beam passes through differentially pumped regions in the TOF section, and enters the detector chamber where the atoms are ionized by electron bombardment. The ions produced then travel through a quadrupole mass spectrometer set to pass the He mass, and the selected ions are counted by standard electron-pulse counting techniques. Helium atoms not ionized in the electron bombardment enter a separately pumped sump chamber and are removed.

The single-crystal KLT samples studied in the experiments reported here were produced by one of us (L.A.B.) at the Oak Ridge National Laboratory. Samples with three different lithium doping concentrations, nominally 2%, 4%, and 7%, were used. The bulk lattice parameters for the KLTs are 3.99 Å,[21] about the same as for KT, and the variations in the parameters are smaller than the ∼1% resolution of the HAS instrument. Bulk phase transition temperatures for KTN have been determined over the full range of niobium doping levels, from KT to potassium niobate.[33] The phase transition temperatures for KLT are known only for a few low-concentration samples, and primarily only for the cubic/paraelectric phase to the tetragonal phase. The cubic/paraelectric to tetragonal phase transitions for 1.5% Li, 3.5% Li, and 5% Li are at 30, 55, and 75 K, respectively.[9] Sample temperatures in the experiments in this paper were kept well above any of the known transition temperatures and, hence, the bulk samples were presumed to be in the cubic/paraelectric phase.

Each sample was mounted on a manipulator equipped for alignment with an x, y, z translational stage, two rotational adjustments, and a tilting stage. The manipulator can also cool or heat the samples over the range of approximately 80 to 350 K. After mounting a sample, the chamber was evacuated and baked. The sample was then cleaved *in situ* by a jaws type of cleaver, usually at room temperature (nominally 300 K) and at a base pressure of about 1×10^{-9} mbar. This pressure was higher than that obtained for the earlier HAS experiments reported from this laboratory on KT and KTN. For this reason, the surface quality deteriorated substantially over a period of several hours compared to about two weeks for the earlier work. Consequently, the sample was cleaved relatively frequently to produce high-quality surfaces for these experiments.

Two types of elastic helium scattering studies were carried out. The first, angular distributions (ADs), are measurements of the He diffraction intensity as the manipulator holding the sample is rotated by a stepping motor, i.e., measurements of He scattering intensity versus θ_i.[22,23] These are most informatively plotted as the scattering intensity versus ΔK, the difference in surface-parallel wave-vector components of the scattered and incident helium beams. The relation between ΔK and θ_i is given by $\Delta K = k_f \sin\theta_f - k_i \sin\theta_i$. For elastic scattering in this instrument, ΔK is given by[23,26]

$$\Delta K = \sqrt{2} k_i \cos(\theta_i + 45°). \quad (1)$$

Here, k_f and k_i are the magnitudes of the scattering and incident He wave vectors, respectively, and for elastic scattering $k_i = k_f$. By varying the temperature of the sample holder, the ADs can be measured as a function of surface temperature. ADs provide information about the surface lattice parameters, reconstruction, and metastable behavior after cleaving (see following). The condition for Bragg diffraction is $\Delta\mathbf{K} = \mathbf{G}_{mn}$, where $\mathbf{G}_{mn}$ is a surface reciprocal lattice vector.[34]

Drift spectra (DSs) are the second type of experiment.[26] These are measurements of the specular reflection intensity as the nozzle temperature is allowed to drift in a controlled fashion from high to low temperature or from low to high temperature. Since He atom wave vectors can be determined from the nozzle temperatures by experimental calibration, a DS measures the dependence of the He specular peak intensity on the He wave vector. The intensity varies due to interference in the scattering of a He atom from terraces at different surface heights. The Fourier transform (FT) of intensities in a DS with respect to the magnitude of the difference in surface normal wave vectors Δk_z thus provides information about the distribution of step heights separating terraces at the surface.[35] In this HAS instrument,

$$\Delta k_z = \sqrt{2} k_i \sin(\theta_i + 45°). \quad (2)$$

III. EXPERIMENTAL RESULTS

A. Metastable behavior after cleaving

After cleaving a KLT crystal, the manipulator has to be adjusted to align the sample in the proper orientation to carry out the He scattering experiments. This can typically take 10 minutes to an hour. In the experiments reported here, as soon as the sample was aligned, a series of AD scans was

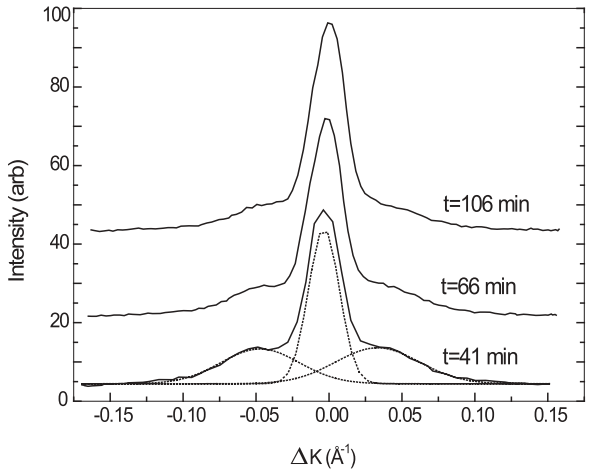

FIG. 1. High-resolution AD measurements in the region about the specular beam from the (001) surface of a 4% Li-doped KLT sample in the ⟨100⟩ azimuth at 300 K taken at the times after the cleave, as indicated. The shoulders flanking the specularly reflected helium beam decrease with time from the sample cleaving in the three curves shown. The relative intensities of the specular peak and the metastable shoulders have been obtained by fitting each measured AD with three Gaussians as shown in the lowest curve. The background has been removed for this analysis. Plots of these intensities against time after cleaving are presented in Fig. 5. Note that the curves have been offset for clarity.

taken in the region of the specular reflection as a function of time after cleaving. Three of these are shown in Fig. 1, with the intensities plotted against ΔK for a 4% Li-doped sample. It is apparent from the decreasing intensities of the shoulders about the specular peak that the surface is changing over a period of an hour or so. This metastable behavior is generally similar to that found in HAS experiments with KT.[22,23,29] The most striking difference is the rapid growth of the specular peak for KT,[29] whereas in this work (Fig. 1), the specular peak starts relatively large and grows only modestly. Further, distinct metastable peaks flanking the true specular beam were not observed. However, it was possible to quantify the changes with time in the signal widths by fitting the measured signal to three Gaussians, as shown in the figure. The integrated intensities of the metastable flanking portions could then be plotted against the time elapsed from cleaving. This procedure is elaborated in Sec. IV. In these experiments, the positions of the "metastable" peaks were found to be at $\Delta K = \pm 0.040$ Å^{-1}. Similar behavior was also observed for the 2% and 7% Li-doped samples.

One should note that the experimental conditions for the metastable behavior results reported here differ somewhat from those in the earlier studies on KT.[29] The higher base pressures, and consequently faster deterioration of the surface quality as mentioned in the previous section, may affect the rate of change of surface structure. To minimize adsorption of background gas, similarly, the temperature of the sample in these studies was maintained at 300 K rather than at 190 K in the previous work. Finally, the He wave vectors in the experiments on KT essentially satisfied the "out-of-phase" condition for the 4.0-Å step height, whereas in these

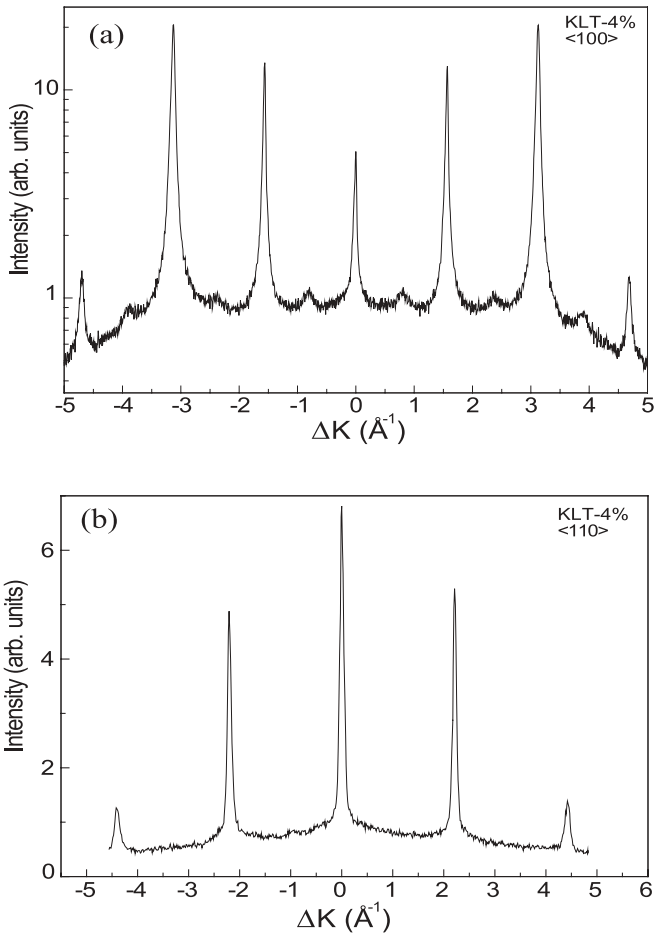

FIG. 2. AD measurements of helium scattering from the (001) surface of a 4% Li-doped KLT sample in the ⟨100⟩ azimuth at surface temperature 300 K (upper panel) and in the ⟨110⟩ azimuth at surface temperature 190 K (lower panel). Sharp Bragg diffraction peaks are seen in both panels which correspond to a square 4-Å surface mesh, which is the same as the cubic bulk lattice parameter. However, in the ⟨100⟩ azimuth, one also sees the small and broad half-order diffraction peaks that suggest that a small fraction of the surface has reconstructed into a (2×1) structure. The data in panel (a) are plotted on a logarithmic scale to display the half-order peaks more prominently.

investigations the He wave vectors lay between the "in-phase" and "out-of-phase" conditions.

B. Angular distributions

Full angular distribution measurements, from approximately $20^\circ \leqslant \theta_i \leqslant 70^\circ$, in the ⟨100⟩ and ⟨110⟩ high-symmetry azimuths are shown in Fig. 2 for scattering from a 4% Li-doped sample. Sharp peaks are observed that match the Bragg diffraction conditions for a square surface unit mesh with dimensions of 4.0 Å, which lies within the resolution of this HAS instrument for the dimensions of the bulk cubic unit cell. The sharp diffraction peaks appearing in the ADs, therefore, are just what one would expect after cleaving the sample to yield a (001) surface.

However, in Fig. 2(a), one also sees half-order diffraction peaks which are quite small and broad compared to the

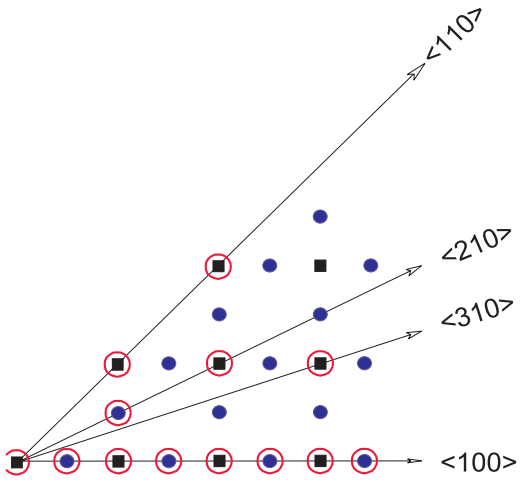

FIG. 3. (Color online) Reciprocal lattice plot showing the reciprocal lattice points corresponding to a (1×1) surface mesh (solid squares) and additional points from a (2×1) and (1×2) mesh (solid circles). The arrows and labeled azimuths show the directions that have been measured in AD experiments. The circled points identify Bragg peaks seen in these diffraction measurements.

integer-order peaks. As in the He diffraction experiments on KT(001) and on the several KTN(001) surfaces reported previously, the half-order peaks suggest that a portion of the surface has reconstructed into small (2×1) domains.[22,23,25,26] The half-widths of these peaks suggest that the domain dimensions are roughly 60 Å. In the previous work, it was suggested that these domains are the surface manifestation of the polar nanoregions observed in the bulk of these materials arising from crystal defects.[6,7,10,12,13,16–21]

The appearance of the half-order peaks in the ADs for KLT differs from those observed for KT and the KTNs in one notable aspect. In these experiments, the peaks were found to grow in over a period of 30 to 60 min in ADs taken on samples cleaved and kept at room temperature. In the work on KT and KTN, half-order diffraction peaks were never found for samples kept at room temperature, even after several days. As in the previous work, however, these diffraction peaks were seen to disappear over a few hours when the samples were warmed in these experiments to 325 K. This behavior was similar for all the 2%, 4%, and 7% Li-doped samples that were investigated.

AD experiments were carried out in other azimuths for some of the samples to verify the structure of the domains as (2×1); namely, in the $\langle 210 \rangle$ and $\langle 310 \rangle$ azimuths. As expected for (2×1) domains, half-order diffraction peaks were observed in $\langle 210 \rangle$, but not in $\langle 310 \rangle$. Figure 3 shows the expected reciprocal lattice points for a (2×1) structure as solid dots. Dots with circles indicate the reciprocal lattice points that were observed in the He diffraction studies.

C. Drift spectra

Examples of DSs for the 4% Li-doped samples are shown in Fig. 4 along with their respective FTs. Because the range of Δk_z available to this instrument is limited to approximately 9–16 Å^{-1}, the FTs are rather broad. To aid in interpretation of the step-height distributions at the surface that give rise to the DSs, the FTs have been fit to Gaussians. The dominant result shows a large peak at 4 Å and a smaller one at 8 Å; a few DSs also show a small peak at 6 Å. As noted above, cleaving KLT samples with a unit cell of 4 Å might be expected to produce a one-to-one mix of KO/ LiO and TaO_2 terraces. These would manifest in DSs as step heights at the surface in multiples of 2 Å. This result was seen, in effect, in experiments on $KMnF_3$ as cleaving this perovskite produces only KF and MnF_2 terraces.[28] The predominant result of 4-Å steps, and multiples of 4-Å steps, is consistent with the explanation for the metastable behavior around the specular beam observed soon after cleaving, as discussed in the following.

IV. DISCUSSION

A. Metastable behavior

The time-dependent changes in the scattering near the specular reflection angle in the experiments on KT were ascribed to the migration of K and O ions to the surface from the near-surface bulk. Cleaving KT should produce an equal distribution of complementary KO and TaO_2 regions. The observation of dominance of 4-Å steps from the DSs suggest that only one of these remains after some time. If the K and O ions migrate to the surface, the surface should evolve to becoming mainly KO.[30]

A treatment by Croset and de Beauvais for scattering from a surface made up of terraces separated by a single step height and having a distribution of terrace lengths could be adapted to this picture of the evolving KT surface.[31] Correlating the predicted scattering intensities with the measurements gave a good fit to the time dependence observed.[29] The data suggest that a similar approach could be applied to the experiments on KLT reported here.

The simplest model for the migration of ions to the surface assumes that the rate of change of coverage by the ions is proportional to the area of the surface not yet covered. If we let Θ be the coverage of the surface by K^+ and O^{2-} ions, then the cleave produces a surface with $\Theta = \frac{1}{2}$. If the surface were fully covered by K^+ and O^{2-} ions, then Θ would equal 1. The rate of change of the coverage in this model is given by

$$\frac{d\Theta}{dt} = \kappa(1 - \Theta) \tag{3}$$

with the rate constant κ. Integrating this equation with $t = 0$ and $\Theta = \frac{1}{2}$ initially at the cleave yields

$$\Theta(t) = 1 - \tfrac{1}{2}\exp(-\kappa t). \tag{4}$$

The Croset and de Beauvais treatment predicts that the intensity of the scattering at $\Delta K \neq 0$ should be given by a function of the form[29]

$$I_{\text{shoulder}}(t) = C_1 + C_2 \cos\left[2\pi\left(\Theta(t) - \tfrac{1}{2}\right)\right], \tag{5}$$

where we determined C_1 and C_2 by fitting the data. Combining this with Eq. (4), one expects the intensity of the metastable signal flanking the specular beam to decrease according to

$$I_{\text{shoulder}}(t) = C_1 + C_2 \cos\{\pi[1 - \exp(-\kappa t)]\}. \tag{6}$$

For the specular beam $\Delta K = 0$, and Croset and de Beauvais report that the intensity should be the sum of a singular term

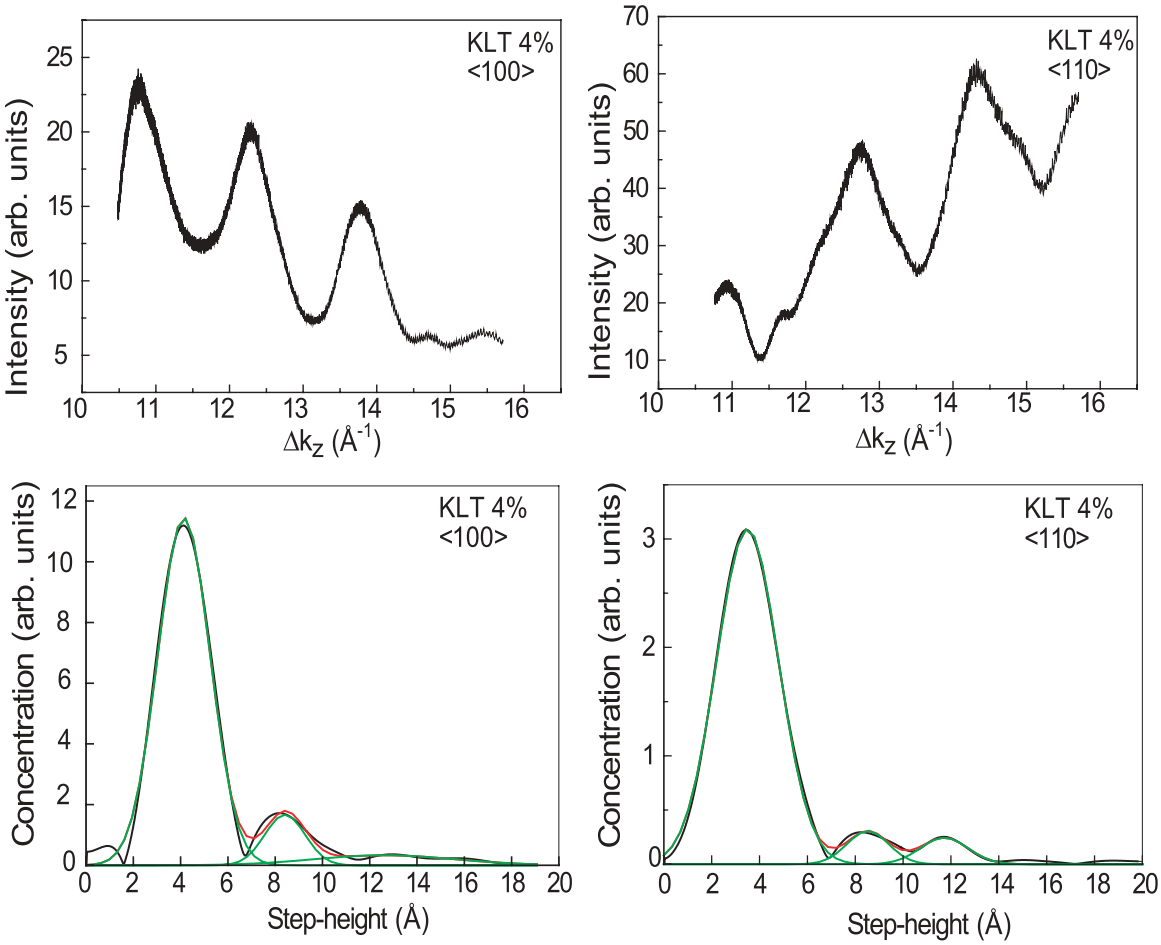

FIG. 4. (Color online) Drift spectra measurements from the (001) surface of a 4% Li-doped KLT sample in the ⟨100⟩ azimuth at surface temperature 190 K (left upper panel) and in the ⟨110⟩ azimuth at surface temperature 300 K (right upper panel). Their respective Fourier transforms are shown in the lower panels. The small range of Δk_z covered in the DS experiments lead to broad step-height distributions in the FTs. Gaussian fits to the FTs, as shown in the lower panels, indicate that the principal step height on the surface is 4 Å with a smaller probability for steps of 8 Å.

plus a nonsingular term.[31] At $\Delta K = 0$, the nonsingular term should be a constant. In Ref. 29, we noted that when k_i satisfied the out-of-phase condition, the singular term varied as $I_s \propto [\Theta(t) - \frac{1}{2}]^2$. Although this condition is not as well satisfied for the KLT experiments, we nevertheless obtained good results by fitting the time dependence of the specular beam with a function of the form

$$I_{\text{specular}}(t) = C_3 + C_4 \left(\Theta(t) - \tfrac{1}{2}\right)^2 . \tag{7}$$

From the kinetic model, Eq. (7) becomes

$$I_{\text{specular}}(t) = C_3 + C_4 \left(\tfrac{1}{2} - \tfrac{1}{2}\exp(-\kappa t)\right)^2 . \tag{8}$$

Figure 5 shows data from these experiments, along with data obtained previously on KT for comparison,[29] plotted as suggested by Eqs. (6) and (8). The solid lines are the fits to the data which are rather good. As shown in Fig. 5, the scaling constants C_1 and C_2 for the KLT satellites are 1344 and 534, respectively; for KT, they are 1157 and 586, respectively. The scaling constants C_3 and C_4 for the KLT specular peak are 1537 and 1375, respectively; for KT, they are 88.7 and 2054, respectively. For the satellites and specular peaks of KLT, $\kappa = 0.018$ min^{-1}, whereas for KT, $\kappa = 0.036$ min^{-1}. We can not offer an explanation at this time for the factor of 2 difference in κ values for KT and KLT. Although the relative change in specular intensity was much larger for KT over the entire range of the data, the change during overlapping times after cleaving is consistent with the observed difference in κ. As mentioned in Sec. III A, there were several experimental differences between the earlier results for KT and the present results for KLT, including the rate of surface contamination, the surface temperature, and the He wave vectors used which may have influenced the measured value of κ.

The data can also be fit by assuming that the increasing coverage by the migrating ions $(\Theta - \frac{1}{2})$ varies with time by a power law; that is, $(\Theta - \frac{1}{2}) = C_5\, t^n$. In a previous paper, we were able to fit the data adequately by having $n = \frac{1}{2}$.[29] However, a power law introduces an extra free parameter into Eqs. (6) and (8). We prefer the model given by Eqs. (3) and (4) because of its more natural interpretation in terms of simple kinetics and because it requires only three free parameters to fit the data in Fig. 5(b), rather than four, and only two free parameters to fit the data in Fig. 5(a).

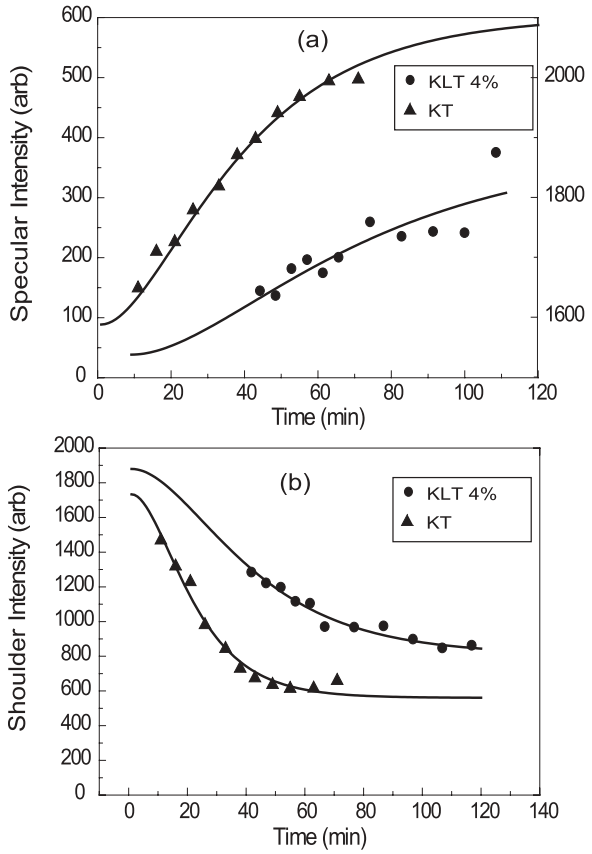

FIG. 5. (a) The time dependence of the specular beam intensities for the 4% KLT samples obtained in these experiments (solid circles) and, for comparison, the specular intensities for KT reported previously (solid triangles) (Ref. 29). The solid curves through the data are from the model given by Eq. (8) in the text. Note that the ordinate scale on the left is for KT and that on the right is for KLT; the ordinate scaling of the data and model curves has been adjusted for convenient viewing. (b) The time dependence of the average intensities of the metastable shoulders, as shown in Fig. 1, are presented for the 4% KLT sample (solid circles) and for the similar data reported previously for the metastable peaks observed after cleaving KT (solid triangles) (Ref. 29). The solid curves are fits using the form of Eq. (6) in the text. Note that the ordinate scaling of the data and model curves has been adjusted for convenient viewing. The rate constants κ were determined by fits to the metastable shoulder data. From the KLT points, κ is found to be 0.018 min^{-1} and for KT 0.036 min^{-1}. The rate constants κ used for the model curves in (a) were those determined in fitting the data for (b).

B. Angular distributions

The sharp integer-order diffraction peaks as shown in Fig. 2 indicate that the surface is well ordered over regions with dimensions larger than the correlation length of the He beam. For the beam velocity distribution and angular spread of this instrument, this length is roughly 300 to 500 Å. The significant background, however, suggests that these well-ordered regions are smaller than those for cleaved alkali halide surfaces, which are estimated to be in the range of several thousand ångstroms. With the low levels of Li doping in the crystals prepared for these studies at the temperatures that were explored, we expect that all of the samples remain in the cubic/paraelectric phase in these experiments. The integer-order diffraction peaks are found at angles satisfying the Bragg diffraction condition consistent with this assumption. As indicated above, the widths of the much smaller half-order peaks suggest approximately 60-Å surface domains, much smaller than the He beam correlation length.

In the HAS experiments on KT and the KTN (001) surfaces, He diffraction from samples cleaved at room temperature and then cooled to and kept at 190 K never showed half-order diffraction peaks. However, when these samples were cooled to much lower temperatures (<100 K) and then warmed to 190 K or higher, half-order peaks appeared in subsequently measured ADs. These peaks were also observed to "grow in," after cleaving at room temperature, over a period of about two to three days for samples cooled to and kept at about 220 K and over a few hours for samples between 250–270 K. Samples kept at room temperature, however, did not show evidence of the (2×1) domains even after several days. Further, for samples having (2×1) domains, warming to about 330 K caused the half-order diffraction peaks to disappear over a period of a few hours. In the KLT samples studied here, the (2×1) domains form even at room temperature implying that the slight doping with Li^+ ions somehow extends the range of stability of these domains.

In the KTN investigations,[25,26] it was noticed that samples with greater doping levels of niobium ions appeared to yield smaller half-order peak intensities relative to the intensities of the integer-order peaks. Pure KT crystals do not undergo any phase transitions, but substitution of Nb^{5+} ions for Ta^{5+} ions allows the crystal to undergo several ferroelectric reconstructions of the cubic KT lattice as the temperature is lowered. Since the (2×1) domain structure implies an antiferroelectric arrangement of the surface net, it was thought that Nb doping might inhibit the formation of (2×1) domains. That is, increasing the Nb concentration would lead to decreasing (2×1) domains and therefore smaller and broader half-order peaks in the ADs. The substitution of Li^+ ions for some K^+ ions has a similar effect in that it allows the crystal to undergo ferroelectric phase transitions. However, this substitution, even at the low concentration levels in these experiments, appears to promote the formation of the (2×1) antiferroelectric domains at higher temperatures.

The formation of polar nanoregions in the bulk has been ascribed to the polarizing fields associated with defects. If the proposed migration of K^+ and O^{2-} ions to the surface discussed above is correct, then as they migrated, defects should be left in the near-surface region of the sample. Such polarizing defects could produce antiferroelectric displacements at the surface, the stability of which would depend on the sample temperature. The data suggest that the Li^+ ion substituting for some K^+ ions promotes antiferroelectricity at higher temperatures. This may be because a Li^+ ion at the surface can occupy one of several off-center positions, thereby enhancing the polarizing electric field.[12]

C. Drift spectra

The FTs of all the measured drift spectra for KLT, as illustrated in Fig. 4, show that the most probable step height separating terraces is 4 Å, the unit-cell dimension. This is consistent with the discussion above that migration of ions from the near surface to the surface has produced a KLT (001) surface which

is predominantly KO. The next most probable step height, from the FTs, is 8 Å, a two-unit-cell step. Again, this is consistent with the migration picture of the ion dynamics after cleaving. In some DSs, the FTs also show a small fraction of 6-Å steps. This would imply that some of the TaO_2 portion of the surface remains uncovered. For the KT and the KTN investigations, the DSs did not reveal significant FT intensity for 6-Å steps.

Two important questions arise from these results, especially as compared with the similar experiments with $KMnF_3$ in which the cleaved (001) surface appeared to be composed of KF and MnF_2 terraces.[28] First, He scattering can not identify the chemical identity of the surface species. We have relied on the results of high-temperature studies that show the lower charged ions, potassium (lithium) and oxygen here, migrating from the bulk to the surface.[30] Other experiments need to be carried out to verify that the stable surface in KT, KTN, and KLT is essentially a KO surface. Then, it is still an open question as to whether the difference in the behaviors of the KTs versus $KMnF_3$ after cleaving is that the cleaved surface of the KTs is formally charged (KO or LiO is formally -1, TaO_2 or NbO_2 is formally $+1$), whereas for $KMnF_3$ it is not (KF and MnF_2 have no formal charge); or, is the difference due to the stronger ionic bonding of the smaller fluoride versus the larger oxide, which inhibits the ionic migration.

Recent experiments on formally charged perovskite interfaces reveal the formation of a "polar catastrophe" at the interface that is relieved by the migration of electrons.[1–3,36] This results in a range of remarkable interfacial phenomena that include superconductivity and ferromagnetism. Similar conditions developing at the cleaved surfaces of the potassium tantalates may be responsible for ionic migration to the surface that is manifested in the metastable behavior observed soon after cleaving and in the measured drift spectra.

V. CONCLUSION

Recent work exploring the behavior at interfaces of complex oxides depends on understanding the composition and structure of the surfaces of these materials. The experiments reported here show the following:

(1) The surfaces of these KLT perovskites undergo dynamic rearrangement for more than an hour after cleaving single-crystal samples. The time dependence of the rearrangements is well represented by combining a simple kinetic model with the scattering treatment by Croset and de Beauvais.[31] Based on results of high-temperature experiments in other laboratories, the rearrangements are ascribed to the migration of K^+ (Li^+) and O^{2-} ions from the near surface to the surface.

(2) The drift spectra show that the predominant step height separating terraces at the surface is 4 Å, which is consistent with the migration of ions, as above. This suggests that the stable surface is, for the most part, a KO(LiO) surface.

(3) Further, for the family of perovskites KT, KTN, and KLT, the cleaved (001) surface may be partially composed of domains with (2×1) unit mesh, depending on the sample temperature and composition.

(4) The dynamic effects observed for these surfaces produced by cleaving may arise because they are not electrically neutral when initially formed. Ionic reconstruction and electronic modification may have to occur to produce energetically stable surfaces.

ACKNOWLEDGMENTS

The authors wish to acknowledge the assistance of S. Barton in some of these experiments. We also wish to acknowledge the support of this research in the past by the Center for Materials Research and Technology (MARTECH) at the Florida State University and by the US Department of Energy through Grant No. DE-FG02-97ER45635. Data analysis by one author (F.A.F.) was facilitated by a Faculty Research Seed Grant from Valdosta State University. Research at the Oak Ridge National Laboratory for one author (L.A.B.) is sponsored by the US Department of Energy, Basic Energy Sciences, Material Sciences and Engineering Division.

*Present address: Gulf Coast State College, Panama City, FL 32401.
†rip@phy.fsu.edu

[1] Pavlo Zubko, Stefano Gariglio, Marc Gabay, Philippe Ghosez, and Jean-Marc Triscone, Annu. Rev. Condens. Matter Phys. **2**, 141 (2011).
[2] H. W. Hwang, Y. Iwasa, M. Kawasaki, B. Keimer, N. Nagaosa, and Y. Tokura, Nat. Mater. **11**, 103 (2012).
[3] See, for example, Pouya Moetakef, Tyler A. Cain, Daniel G. Ouellette, Jack Y. Zhang, Dmitri O. Klenov, Anderson Janoti, Chris G. Van de Walle, Siddharth Rajan, S. James Allen, and Susanne Stemmer, Appl. Phys. Lett. **99**, 232116 (2011).
[4] S. R. Phillpot, M. Sepliarsky, M. G. Stachiotti, R. L. Migoni, and S. K. Streiffer, J. Mater. Sci. **40**, 3213 (2005).
[5] F. Borsa, U. T. Höchli, J. J. van der Klink, and D. Rytz, Phys. Rev. Lett. **45**, 1884 (1980).
[6] V. Trepakov, F. Smutny, V. Vikhnin, V. Bursian, L. Sochava, L. Jastrabik, and P. Syrnikov, J. Phys.: Condens. Matter **7**, 3765 (1995).
[7] J. Toulouse and B. Hennion, Phys. Rev. B **49**, 1503 (1994).
[8] S. R. Andrews, J. Phys. C: Solid State Phys. **18**, 1357 (1985).
[9] P. Doussineau, Y. Farssi, C. Frénois, A. Levelut, K. McEnaney, J. Toulouse, and S. Ziolkiewicz, Europhys. Lett. **21**, 323 (1993).
[10] W. A. Kamitakahara, C.-K. Loong, G. E. Ostrowski, and L. A. Boatner, Phys. Rev. B **35**, 223 (1987).
[11] V. A. Trepakov, M. E. Savinov, S. Kapphan, V. S. Vikhnin, L. Jastrabik, and L. A. Boatner, Ferroelectrics **239**, 305 (2000).
[12] G. Geneste, J-M. Kiat, H. Yokota, Y. Uesu, and F. Porcher, Phys. Rev. B **81**, 144112 (2010).
[13] L. A. Knauss, R. Pattnaik, and J. Toulouse, Phys. Rev. B **55**, 3472 (1997).
[14] J. Toulouse, B. E. Vugmeister, and R. Pattnaik, Phys. Rev. Lett. **73**, 3467 (1994).
[15] U. T. Höchli, K. Knorr, and A. Loidl, Adv. Phys. **39**, 405 (1990).
[16] George A. Samara, J. Phys.: Condens. Matter **15**, R367 (2003).

[17]H. Uwe, K. B. Lyons, H. L. Carter, and P. A. Fleury, Phys. Rev. B **33**, 6436 (1986).
[18]P. DiAntonio, B. E. Vugmeister, J. Toulouse, and L. A. Boatner, Phys. Rev. B **47**, 5629 (1993).
[19]S. Wakimoto, G. A. Samara, R. K. Grubbs, E. L. Venturini, L. A. Boatner, G. Xu, G. Shirane, and S.-H. Lee, Phys. Rev. B **74**, 054101 (2006).
[20]J. Toulouse, P. DiAntonio, B. E. Vugmeister, X. M. Wang, and L. A. Knauss, Phys. Rev. Lett. **68**, 232 (1992).
[21]Hiroko Yokota, Yoshiaki Uesu, Charlotte Malibert, and Jean-Michel Kiat, Phys. Rev. B **75**, 184113 (2007).
[22]Jaime A. Li, Ph.D. thesis, Florida State University, 1999.
[23]Jaime A. Li, E. A. Akhadov, Jeff Baker, L. A. Boatner, D. Bonart, J. Fritsch, S. A. Safron, U. Schröder, J. G. Skofronick, and T. W. Trelenberg, Phys. Rev. B **68**, 045402 (2003).
[24]Thomas W. Trelenberg, Ph.D. thesis, Florida State University, 2001.
[25]T. W. Trelenberg, Rifat Fatema, Jaime A. Li, E. A. Akhadov, David H. Van Winkle, J. G. Skofronick, Sanford A. Safron, F. A. Flaherty, and L. A. Boatner, J. Phys.: Condens. Matter **22**, 304009 (2010).
[26]Rifat Fatema, T. W. Trelenberg, David H. Van Winkle, J. G. Skofronick, S. A. Safron, F. A. Flaherty, and L. A. Boatner, Phys. Rev. B **84**, 144114 (2011).
[27]J. Fritsch and U. Schröder, Phys. Status Solidi **215**, 827 (1999).
[28]J. P. Toennies and R. Vollmer, Phys. Rev. B **44**, 9833 (1991).
[29]Jaime A. Li, E. A. Akhadov, Jeff Baker, L. A. Boatner, D. Bonart, F. A. Flaherty, J. Fritsch, S. A. Safron, U. Schröder, J. G. Skofronick, T. W. Trelenberg, and D. H. Van Winkle, Phys. Rev. Lett. **86**, 4867 (2001).
[30]K. Szot, W. Speier, M. Pawelczyk, J. Kwapulinski, J. Hulliger, H. Hesse, U. Breuer, and W. Quadakkers, J. Phys.: Condens. Matter **12**, 4687 (2000).
[31]B. Croset and C. de Beauvais, Surf. Sci. **384**, 15 (1997).
[32]Rifat Fatema, Ph.D. thesis, Florida State University, 2009, http://etd.lib.fsu.edu/theses/available/etd-04132009-104547/unrestricted/FatemaRDissertation.pdf.
[33]D. Rytz and H. J. Scheel, J. Cryst. Growth **59**, 468 (1982).
[34]G. Brusdeylins, R. B. Doak, and J. P. Toennies, Phys. Rev. B **27**, 3662 (1983).
[35]D. A. Hamburger, A. T. Yinnon, I. Farbman, A. Ben-Shaul, and R. B. Gerber, Surf. Sci. **327**, 165 (1995).
[36]N. Nakagawa, H. Y. Hwang, and D. A. Muller, Nat. Mater. **5**, 204 (2006).